Detection of Early Warning Signals for Self-Organized Criticality in Cellular Automata

Andrey Dmitriev[1,a], Anastasiia Kazmina[1], Victor Dmitriev[1], Yuriy Sanochkin[1], and Evgenii Gradusov[1]

[1] Department of Business Informatics, National Research University Higher School of Economics, Moscow, Russia
[a] E-mail: a.dmitriev@hse.ru

Abstract. Detection the precursors of critical transitions in complex systems is one of the most difficult and still unsolved problems. This problem has not received a final solution, not only for real complex systems, but also for model systems capable to self-organize into the critical state. The presented paper is devoted to early detection of time moments of self-organized critical transitions in cellular automata as a result of the analysis of the time series they generate for a number of grains falling from the grid. It was found that cumulative moments of probability distribution and cumulative scaling exponents are quite informative indicators for early detection of critical transitions. General features of the behavior of indicators when approaching a critical point are established for the time series generated by cellular automata with different rules.
Keywords: Cellular Automata, Sandpile Model, Self-Organized Criticality, Time Series, Probability Moments, Multifractality.

1 Introduction

More than thirty years development of the theory of self-organized criticality (SOC), explaining the emergence of power law for probability density function, 1 / f-noise and long-range spatial and temporal correlation in nonlinear systems far from equilibrium, has led to the emergence of the number of basic models, which have nontrivial scale-invariant dynamics under very simple local rules [1,2]. The basic models of SOC theory are sandpile models [3]. These models have become the most important tool for studying the mechanisms of the appearance of scale-invariant properties and power statistics.

The sandpile model is a conical pile of sand, on the center of which grains of sand are placed one by one. We will assume that the cohesion between grains of sand is large enough and only superficial movement of sand is possible. Then the state of the system is determined by the local slope of the surface of the sand pile (S). If S is small, then the sand is motionless. If S exceeds a certain value S_c, then there is a spontaneous flow of sand η over the surface, which increases continuously with increasing of S. This process corresponds to a second-order phase transition, in which the control parameter is S, the order parameter is η. The value S_c separates subcritical (SubC) phase and supercritical (SupC) phase. A pile of sand in these phases is resistant to small disturbances. On the contrary, the SOC state is highly volatile. Adding just one

grain of sand to a pile in this state can lead to avalanches of sand of any size theoretically.

A fundamentally important property of systems, which are characterized by avalanche-like behavior, is their ability to self-organize into the critical state. In this case, it is not required to fine-tune the parameter S to the value S_c. Such systems are capable to transit to the SOC state spontaneously, which is typical for most real and model complex systems, the behavior of which is determined by the nonlinear local rules.

Scale-invariant properties and power statistics are characteristics not only for the level of the structure of the complex system and its local microscopic interactions, but also for the level of time series generated by such systems [4]. For the sandpile model, such time series are the time series (η_t), which demonstrate the stochastic dynamics of sand grains falling on the surface of the pile. When describing a pile of sand using cellular automata models, η_t is the number of grains falling from the grid. The approach to the study of self-organized critical states of complex systems based on the analysis of generated time series has, at least, one significant advantage. The approach does not require the study of detailed interactions between elements of the real systems. Information about detailed interactions is usually inaccessible for research, for example, for social networks, or inaccessible, for example, for financial networks.

Detection of early warning signals for critical transitions is a challenging task not only for the real complex systems, but also for the model systems. The overwhelming majority of the papers known to us are devoted either to detection of early warning signals associated with the critical slowing down phenomenon [5-8], or to the solution of particular problems of the early warning [9,10]. In these studies, precursors of the critical transitions in real systems were established, which are associated with the change in the autocorrelation function, variance, skewness, and power spectral density of the observed time series when the system parameters approach their critical value.

To our knowledge, however, there is no study that investigates the search for precursors of the SOC transitions not only in real complex systems, but also in model systems, for example, in the self-organized criticality cellular automata. The detection of such precursors as a result of the analysis of the time series for the number of grains falling from the grid is the purpose of our study.

2 Methods

2.1 Time series generated by the cellular automata

It is easy to study the stochastic dynamics of the order parameter (η_t) of the sandpile models using models of cellular automata in grids of size $L \times L$. The parameter η_t is the number of sand grains falling from the grid at time t.

Random integers $z_{i,j}$ are generated in the grid cells to represent the local slope of the sand pile. The cells for which $z_{i,j} \geq z_c$, where z_c is the critical value, are unstable and fall off according to the rules defined for each cellular automata. For the pile of sand, several different variants of the rules for shedding an unstable cell have been proposed. This paper considers six sandpile models, each of which belongs to one of two classes of self-organized critical models: conservative and dissipative models. Models with conservative rules are characterized by the fact that when unstable cells fall, the grains of sand removed from them are redistributed without loss and leave the grid only after reaching its edges. The boundary conditions of such systems are open. In dissipative models, after the shedding of the unstable cell, the number of grains of sand in it is zero. In the case of the supercritical number of sand grains, they are able to leave the grid also within its boundaries.

2.1.1 Conservative systems

Let us consider in more detail the historically very first model, called the BTW-model [11]. Consideration of other models, including dissipative models, is limited to consideration of only the rules for shedding cells.

BTW-model is a cellular automaton on a square grid of size $L \times L$. A grain of sand is randomly added to a randomly selected cell (i, j), increasing the number of grains of sand ($z_{i,j}$) in the cell by one: $z_{i,j} += 1$. As a result, $z_{i,j} \rightarrow z_{i,j} + 1$. If $z_{i,j} \geq 4$, then one grain of sand moves to the four nearest cells: $z_{i\pm1,j\pm1} += 1$. In this case, the number of grains of sand in the cell (i, j) decreases by the value $z_c = 4$: $z_{i,j} -= 4$. The considered movement of sand grains can lead to loss of stability of neighboring cells, and, consequently, lead to the appearance of the avalanche with loss of stability. The introduction of the condition $z_{i,j} -= 4$ leads to the saving of the number of sand grains.

Thus, the rules of the model are as follows:

$$z_c = 4, z_{i,j} -= 4, z_{i\pm1,j\pm1} += 1 \qquad (1)$$

In the Fig. 1 the time series for the number of grains falling from the grid for a 40 × 40 grid of the BTW-model are presented. The rest of the time series looks the same except for the iteration number (or point in time t_c) corresponding to the SOC state. t_c depends on the grid's size: $t_c = 1656$ for 20×20 grid, $t_c = 2171$ for 30×30 grid, $t_c = 3736$ for 40×40 grid, $t_c = 5491$ for 50×50 grid, and $t_c = 8234$ for 60×60 grid.

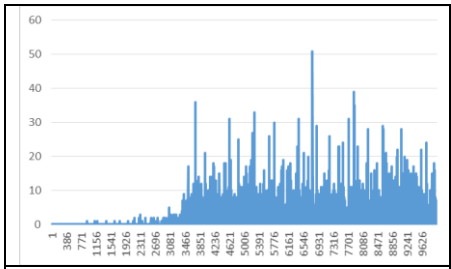

Fig. 1. Time series of the number of grains falling from the grid for the BTW-model

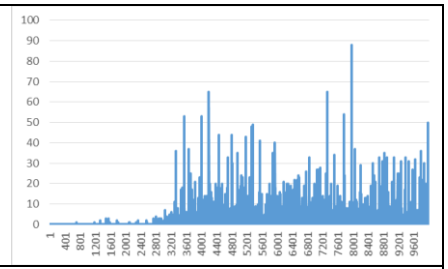

Fig. 2. Time series of the number of grains falling from the grid for the Manna model

Manna model [12] is the stochastic analogue of the BTW-model. The cell (i, j) crumbles as a result of the stability loss, transferring a random number of grains of sand ($\delta_k \geq 0$) to four neighboring cells.

Formally, the rules of the model are as follows:

$$z_c = 4, z_{i,j} -= 4, z_{i\pm1, j\pm1} += \delta_k, \delta_k \geq 0, \sum_k \delta_k = 4 \qquad (2)$$

In the Fig. 2 the time series for the number of grains falling from the grid for a 40 × 40 grid of the Manna model are presented. The rest of the time series looks the same except for the iteration number corresponding to the SOC state. t_c depends on the grid's size: $t_c = 892$ for 20×20 grid, $t_c = 2510$ for 30×30 grid, $t_c = 3335$ for 40×40 grid, $t_c = 5671$ for 50×50 grid, and $t_c = 7625$ for 60×60 grid.

DR-model [13] is the cellular automaton, the rules of which are formulated on a two-dimensional hexagonal lattice. It is a cellular automaton with open boundary conditions on the lower side and periodic boundary conditions on the left and right sides. A grain of sand is randomly added to a randomly selected cell (i, j) of the top layer, increasing the number of grains of sand ($z_{i,j}$) in the cell by one: $z_{i,j} += 1$. When the value in any cell exceeds one, this cell loses stability and crumbles, transferring one grain of sand to the two cells lying below. It is important that the DR-model rules are anisotropic, i.e. the avalanche of sand grains, spreading from the top to the bottom, never affects the same area twice.

Formally, the rules of the model are as follows:

$$z_c = 2, z_{i,j} -= 2, z_{i\pm1, j\pm\frac{1}{2}} += 1 \qquad (3)$$

In the Fig. 3 the time series for the number of grains falling from the grid for a 40 × 40 grid of the DR-model are presented. The rest of the time series looks the same except for the iteration number corresponding to the SOC state. t_c depends on the grid's size: $t_c = 1491$ for 20×20 grid, $t_c = 1821$ for 30×30

grid, $t_c = 3241$ for 40×40 grid, $t_c = 5200$ for 50×50 grid, and $t_c = 7476$ for 60×60 grid.

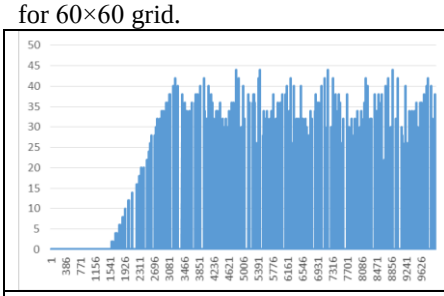

Fig. 3. Time series of the number of grains falling from the grid for the DR-model

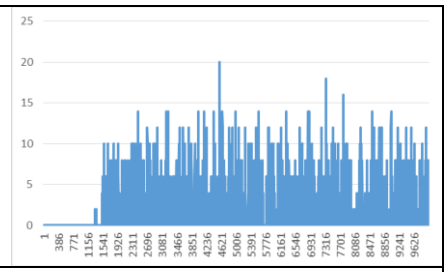

Fig. 4. Time series of the number of grains falling from the grid for the PSV-model

PSV-model [14] is the stochastic analogue of DR-model. The cell (i, j) crumbles as a result of the stability loss, transferring the random number of sand grains ($\delta_{\pm} \geq 0$) to the two cells lying below.

Formally, the rules of the model are as follows:

$$z_c = 2, z_{i,j} -= 2, z_{i\pm1, j\pm\frac{1}{2}} += \delta_{\pm}, \delta_{\pm} \geq 0, \delta_{+} + \delta_{-} = 2 \qquad (4)$$

In the Fig. 4 the time series for the number of grains falling from the grid for a 40 × 40 grid of the PSV-model are presented. The rest of the time series looks the same except for the iteration number corresponding to the SOC state. t_c depends on the grid's size: $t_c = 1$ for 20×20 grid, $t_c = 1$ for 30×30 grid, $t_c = 1$ for 40×40 grid, $t_c = 1$ for 50×50 grid, and $t_c = 1$ for 60×60 grid.

2.1.2 Dissipative systems

The rules of the models considered above are conservative, i.e. when cells are shattered, the grains of sand removed from them are redistributed to neighboring cells without loss. The grains of sand leave the grid only when they reach its edges.

DFF-model [15] is a deterministic cellular automaton with a two-dimensional orthogonal grid of size $L \times L$. The integers in the cells $z_{i,j}$ can be interpreted as the number of grains of sand that can participate in the pouring processes. There is no designated slope direction. If $z_{i,j} \geq 4$, then the cell (i, j) is unstable and overturns. Overturn is zeroing of the number of sand grains in the cell with a simultaneous increase by 1 in the values in four cells that have a common side with this cell.

Formally, the rules of the model are as follows:

$$z_c = 4, z_{i,j} -= 0, z_{i\pm1,j\pm1} += 1 \qquad (5)$$

In the Fig. 5 the time series for the number of grains falling from the grid for a 40 × 40 grid of the DFF-model are presented. The rest of the time series looks the same except for the iteration number corresponding to the SOC state. t_c depends on the grid's size: $t_c = 1$ for 20×20 grid, $t_c = 1$ for 30×30 grid, $t_c = 1$ for 40×40 grid, $t_c = 1$ for 50×50 grid, and $t_c = 1$ for 60×60 grid.

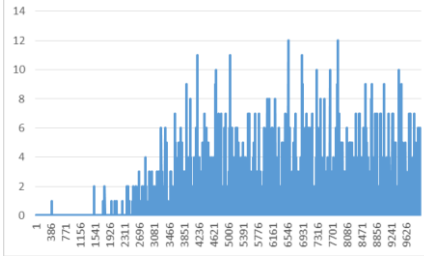

Fig. 5. Time series of the number of grains falling from the grid for the DFF-model

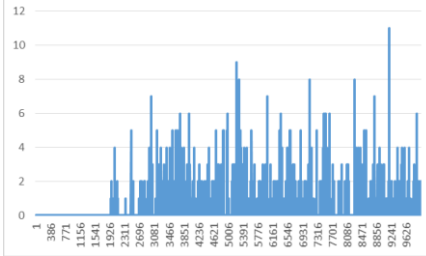

Fig. 6. Time series of the number of grains falling from the grid for the stochastic DFF-model

The stochastic DFF-model with a random number of sand grains (δ_k) in four neighboring cells that have a common side with the cell is characterized by the following rules:

$$z_c = 4, z_{i,j} -= 0, z_{i\pm1,j\pm1} += \delta_k, \delta_k \geq 0, \sum_k \delta_k = 4 \qquad (6)$$

In the Fig. 6 the time series for the number of grains falling from the grid for a 40 × 40 grid of the stochastic DFF-model are presented. The rest of the time series looks the same except for the iteration number corresponding to the SOC state. t_c depends on the grid's size: $t_c = 1$ for 20×20 grid, $t_c = 1$ for 30×30 grid, $t_c = 1$ for 40×40 grid, $t_c = 1$ for 50×50 grid, and $t_c = 1$ for 60×60 grid.

2.2 Moments of probability density function for the time series

Earlier, we proposed the algorithm for detecting the self-organized critical state of the system. The algorithm is based on the analysis of scaling exponents of power laws for probability density function (α), power spectral density (β), and autocorrelation function (γ) for time series generated by SOC systems. The algorithm make it possible to identify the SubC phase and the SupC phase by belonging of α, β and γ to certain intervals. The disadvantage of the algorithm is its applicability only to the analysis of scale-invariant probability density function and the impossibility of its application to the analysis of other heavy-tailed distributions. The heavy-tailed distributions are characteristic for the time intervals of the system evolution, corresponding to its SupC phase. A

famous example of a scale-invariant heavy-tailed distribution is the Pareto distribution.

Therefore, in order to go beyond the limitations of the algorithm associated only with the use of α as the only identifier of the SOC state, the SubC phase and the SupC phase, we used the main moments of probability density function as cumulative indicators.

For detection of early warning signals for self-organized criticality we used the following moments:
first raw moment (or mean) μ,
second central moment (or variance) σ^2,
standardized third moment (or skewness) γ,
standardized fourth moment (or kurtosis) κ.

2.3 Scaling exponents for the time series

Even the description of model time series using the moments of their probability density function is exhaustive only for a very limited number of random processes. For example, realizations of Gaussian processes are fully described by second-order moments. Therefore, apart from the moments, other quantities should be used to describe the time series. These quantities include the scaling exponents for the time series, which determine the fractal dimensions of time series as geometric objects.

The most general approach to the study of scaling exponents of heterogeneous time series is their multifractal analysis. It is sufficient to calculate a single scaling exponent to describe the scale invariance of homogeneous model time series, since such time series demonstrate only one type of singular behavior constant in time. On the contrary, the nature of the singularity of inhomogeneous time series at different points in time may differ; therefore, the description of such time series cannot be performed using only scaling constant. Therefore, multifractal analysis, which allows to provide local analysis of heterogeneous time series, is a more informative approach.

We used multifractal detrended fluctuation analysis (MF-DFA) [16] for making of multifractal analysis of time series generated by self-organized critical cellular automata. The application of this method makes it possible to obtain estimates of the spectrum of scaling constant time series: $\{h(q)\}$.

In short, the algorithm of MF-DFA method is reduced to revealing the power law

$$F(q,s) \propto s^{h(q)} \qquad (7)$$

for the fluctuation function

$$F(q,s) = \left\{ \frac{1}{2N_s} \sum_{\nu=1}^{2N_s} [\mu(\nu,s)]^{\frac{q}{2}} \right\}^{\frac{1}{q}}. \qquad (8)$$

To calculate function (8) from a discrete time series η_i, a fluctuation profile is formed $X_i = \sum_{k=1}^{i}(\eta_k - \overline{\eta})$, which is divided into N_s non-intersecting intervals ν containing the equal number of points s. Further, for each of the intervals, the local trend $x_{\nu,i}$ and the deviation of the fluctuation profile from the local trend $\Delta Y_{\nu,i} = X_{\nu,i} - x_{\nu,i}$ are determined. The value $\mu(\nu, s) = \max \Delta Y_{\nu,i} - \min \Delta Y_{\nu,i}$ for each split interval.

A detailed description of the algorithm of the MF-DFA method, as well as its capabilities and limitations, are presented in the paper [16]. Therefore, we will restrict ourselves by considering the main features of the time series for which the power law is satisfied (7). For multifractal time series at $q > 0$, the main contribution to function (8) is given by the partition intervals ν characterized by large values $\mu(\nu, s)$; at $q < 0$, the main contribution to function (8) comes from the partition intervals ν characterized by small values $\mu(\nu, s)$. For monofractal time series $h(q)$ does not depend on q. This is due to the fact that the behavior of function (8) when changing the scale s is the same for all intervals ν.

3 Results and their Discussion

Cumulative mean and variance, as well as their corresponding time series, are presented in the Fig. 7 and the Fig. 8. These figures show moments and time series for the Manna model. The dimensions of cellular automata are 40 × 40. For other cellular automata and their other grid sizes, the mean and variance behavior are similar.

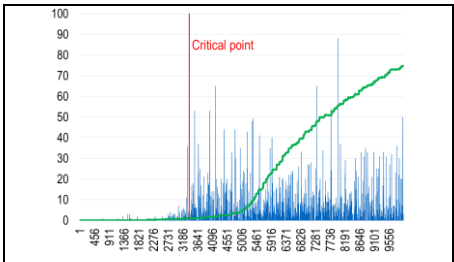

Fig. 7. Cumulative mean for the Manna model

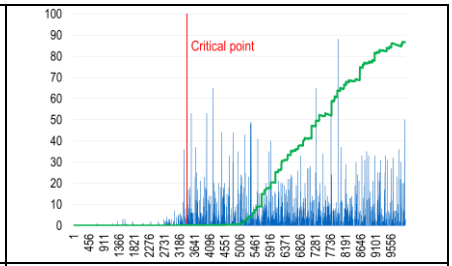

Fig. 8. Cumulative variance for the Manna model

Cumulative mean and variance are not informative indicators characterizing the transition of cellular automata in the SOC state. Indeed, these moments are increasing functions of time and there are no significant changes in them when passing through the SOC state.

Cumulative kurtosis and skewness are quite informative precursors for the transition of cellular automata into the SOC state. The cumulative kurtosis and skewness, as well as their corresponding time series, are presented in the Figures 9 and 10. These figures show the moments and time series for the Manna model. The dimensions of cellular automata are 50 × 50. For other cellular automata and their other grid sizes, the behavior of kurtosis and skewness is similar.

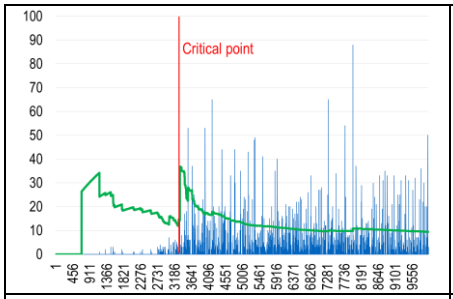

Fig. 9. Cumulative kurtosis for the Manna model

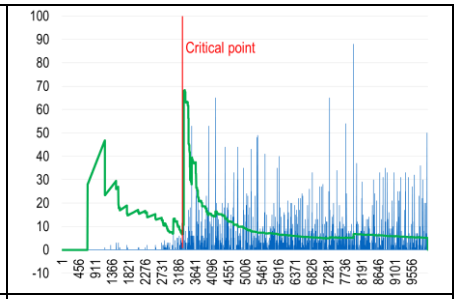

Fig. 10. Cumulative skewness for the Manna model

As the cellular automata approach to the SOC state, a noticeable decrease in kurtosis and skewness is observed up to the critical point. At the same time, a sharp increase in these cumulative moments is observed at the critical point.

The change in the cumulative moments when approaching the critical point has a simple explanation. Mean and variance increase as a result of the increase in the number of grains falling from the grid in the certain time interval $\Delta t_c \in (t, t_c)$ from the SubC phase, preceding the transition of the cellular automaton to the critical state. The decrease in the skewness in the interval Δt_c is also a consequence of the increase in the number of the grains. In this interval, a right-sided asymmetry of the distribution is still observed, characterized by an elongated right "tail," which decreases as the critical point is approached. In other words, the shortening of the right "tail" of the distribution occurs in the interval Δt_c. At the critical point, a sharp lengthening of the right "tail" of the distribution occurs as a result of the accumulation of the number of the grains from the SupC phase. An increase in the number of the grains in the interval Δt_c also leads to a decrease in kurtosis in this interval. The peak of the distribution near the mathematical expectation is sharp for the entire SubC phase, but as the critical point is approached, the peak of the distribution is smoothed out. At the critical point, there is severe increase in the sharpness of the distribution.

In the Fig. 11 the cumulative scaling exponents $h(q)$ at $q = 1, 3, 5$ are shown. The behavior of scaling exponents is similar for all cellular automata and their sizes; therefore, we restrict ourselves by considering only two

automata. The scaling exponents $h(1)$ are shown in blue, in orange – $h(3)$ and in gray – $h(5)$.

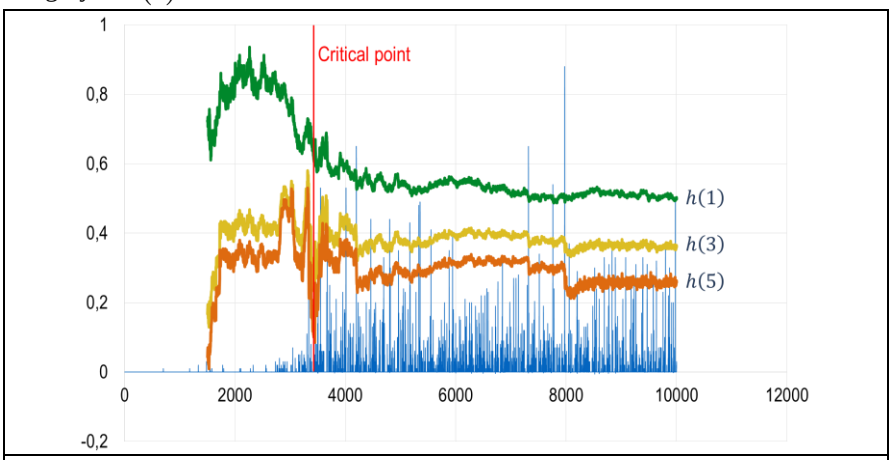

Fig. 11. Cumulative scaling exponents for the Manna model (50×50)

The time series generated by cellular automata are multifractal time series. Moreover, scale invariance in the form (7) is characteristic only for $q > 0$, for $q < 0$ scale invariance is not observed. Therefore, there are only the scaling exponents describing the intervals of time series partitioning ν with large fluctuations. Intervals ν with small fluctuations are not typical for the studied time series.

As approaching to the critical point, the distance between the points $h(q_i) = |h(1) - h(3)| + |h(3) - h(5)|$ decreases and is the smallest at the critical point. In the SupC phase, the distance between the points is almost independent of the iteration. All this is demonstrated in the Figure 11. Recall that for the Manna model (50 × 50) $t_c = 5671$.

Thus, the moments of probability density function, primarily γ and κ, as well as the scaling exponents $h(q)$, can be used as indicators of early warning for the SOC state in cellular automata.

Conclusions

Analysis of the behavior in time of moments and scaling exponents made it possible to provide early detection of the self-organized critical state in cellular automata. For such the early detection, it is sufficient to carry out the statistical and multifractal detrended fluctuation analysis of time series for the number of grains falling from the grid generated by cellular automata.

The results obtained allow us to make the following conclusions:

(1) Self-organized critical cellular automata generate multifractal time series, in which subcritical and supercritical phase, and self-organized criticality state can be distinguished.
(2) The most informative indicators of early detection of self-organized criticality state are cumulative skewness and kurtosis.
(3) Multifractality of time series for number of grains falling from the grid makes it possible to use cumulative scaling exponents as indicators of early detection of self-organized criticality state.

In conclusion, we briefly consider the possible practical applications of the use of the proposed indicators for early detection of critical states. If real systems are able to self-organize into the critical state, then the cumulative moments of probability distribution and the cumulative scaling exponents can be used as early warning indicators for critical states. Self-organized criticality is characteristic of phenomena and processes of a very different nature: solar flares, earthquakes, floods, forest fires, the emergence and extinction of species, demographic, ecological, economic, social, informational processes. Early detection of the critical state means predicting the critical moment in time after which the system behaves in an unpredictable manner. In this case, the system is in the supercritical phase, which is characterized by avalanche-like dynamics.

Acknowledgments

The work is an output of a research project implemented as part of the Basic Research Program at the National Research University Higher School of Economics (HSE University). This research has been conducted within the fundamental research project “Transformation of marketing strategies of customer-oriented business in the context of the global digital economy” as a part of the HSE Graduate School of Business Research Program in 2021-2022 (Protocol No.23 dd 22.06.2021 of the HSE GSB Research Committee).

References

1. P. Bak, C. Tang, and K. Wiesenfeld. Self-organized criticality: An explanation of the 1/f noise. Phys Rev Lett, 59, 381, 1987.
2. D. Dhar. Theoretical studies of self-organized criticality. Physica A, 369, 1, 29-70, 2006.
3. M. Creutz. Self-Organized Criticality and Cellular Automata. In: Meyers R. (eds) Encyclopedia of Complexity and Systems Science. Springer, Berlin, 2018.
4. A. Dmitriev and V. Dmitriev. Identification of Self-Organized Critical State on Twitter Based on the Retweets’ Time Series Analysis. Complexity, 2021, Article ID 6612785, 2021.
5. M. Scheffer et al. Early-warning signals for critical transitions. Nature, 461, 53-59, 2009.
6. C. Diks, C. Hommes and J. Wang. Critical slowing down as an early warning signal for financial crises? Empirical Economics, 57, 1201-1228, 2019.

7. Z. Zhang, Y. Li, L. Hu, C. Tang and H. Zheng. Predicting rock failure with the critical slowing down theory. Engineering Geology, 280, 105960, 2021.
8. V. Dakos et al. Methods for Detecting Early Warnings of Critical Transitions in Time Series Illustrated Using Simulated Ecological Data. PLoS ONE, 7, 7, e41010, 2012.
9. J. J. Lever et al. Foreseeing the future of mutualistic communities beyond collapse. Ecology Letters, 23, 2-15, 2020.
10. L. Zhao et al. Multifractality and Network Analysis of Phase Transition. PLoS ONE, 12, 1, e0170467, 2017.
11. P. Bak, C. Tang, and K. Wiesenfeld. Self-organized criticality. Phys. Rev. A, 38, 1, 364-374, 1988.
12. S. S. Manna. Two-state model of self-organized criticality. J. Phys. A, 24, 7, 363-639, 1991.
13. D. Dhar and R. Ramaswamy. Exactly solved model of self-organized critical phenomena. Phys. Rev. Lett., 63, 16, 1659-1662, 1989.
14. R. Pastor-Satorras and A. Vespignani. Universality classes in directed sandpile models. J. Phys. A, 33, 3, 33-39, 2000.
15. H. J. S. Feder and J. Feder. Self-organized criticality in a stick-slip process. Phys. Rev. Lett., 1991. 66, 20, 2669-2672, 1991.
16. E. A. F. Ihlen. Introduction to multifractal detrended fluctuation analysis in Matlab. Front. Physio., 3, 141, 2012.